

Alloy-Stabilized Semiconducting and Magnetic Zinc-Blende Phase of MnTe

Su-Huai Wei and Alex Zunger

Solar Energy Research Institute, Golden, Colorado 80401

(Received 2 January 1986)

While MnTe has the stable NiAs structure with a direct band gap of 1.30 eV and a Mn-Te bond length of 2.92 Å, extrapolation of the data for the zinc-blende alloy $\text{Cd}_{1-x}\text{Mn}_x\text{Te}$ to $x = 1$ suggests an alloy-stabilized MnTe phase with very different properties: a band gap of ~ 3 eV and a Mn-Te bond length of 2.73 Å. We model the structural, magnetic, and electronic properties of such a hitherto unknown zinc-blende-like MnTe phase through spin-polarized total-energy calculations, and report its unusual properties in both ferromagnetic and antiferromagnetic spin ordering.

PACS numbers: 61.55.Hg, 71.25.Tn, 75.50.Dd, 75.50.Ee

For the vast majority of bulk solid solutions of isovalent binary AC and BC semiconductors, neither the AC nor the BC sublattices alter in the alloy the symmetry of their Bravais lattices.¹ Such is the case for most pseudobinary IV-IV, III-V, II-VI, and I-VII isovalent alloys, which, despite substitutional disorder¹ or tendencies to order,² retain in solution their diamond-like, zinc-blende, wurtzite, and rocksalt substructures, respectively. In addition to these ("type I") alloys, there exists a smaller class (denoted here as "type II") of semiconductor alloys which, as a function of composition x , undergo a transition from one structure to another, where *both* structural forms are known to exist in the phase diagrams of the isolated AC and BC crystals. Such are, for example, the alloys $(\text{CdS})_x(\text{ZnSe})_{1-x}$,³ $(\text{CdS})_x(\text{ZnS})_{1-x}$,⁴ $(\text{CdSe})_x(\text{CeTe})_{1-x}$,⁵ and $(\text{CdSe})_x(\text{HeSe})_{1-x}$,⁶ which transform at some critical composition from the wurtzite to the zinc-blende structure. Interestingly, there exists a third, yet smaller class of alloys (denoted here as "type III") whose observed properties as a function of composition suggest that one component acquires a fundamentally new Bravais lattice, hitherto unknown to exist in its own phase diagram. Such are the mag-

netic semiconductor alloys of MnS, MnSe, and MnTe with a II-VI compound.⁷ While unusual structural forms of alloys have been known to form in extreme nonequilibrium growth methods⁸ and in epitaxial forms,⁹ it is remarkable that alloy-stabilized phases with no counterpart in the phase diagram of the constituent components can be formed in *bulk equilibrium growth*. We first demonstrate from the data that such an unusual, alloy-stabilized zinc-blende phase is likely to exist in $\text{Cd}_{1-x}\text{Mn}_x\text{Te}$ alloys, and then describe its structural, electronic, and magnetic properties through first-principles spin-polarized total-energy and band-structure calculations.

MnTe crystallizes below 1040°C in the hexagonal NiAs structure¹⁰ (NaCl structure at higher temperatures¹⁰) with a direct band gap¹¹ of $E_g(\text{MnTe}) = 1.30$ eV and bond length¹⁰ $R(\text{Mn-Te}) = 2.92$ Å. Zinc-blende CdTe has a low-temperature gap¹² $E_g(\text{CdTe}) = 1.59$ eV and bond length¹³ $R(\text{Cd-Te}) = 2.80$ Å. The solid lines in Fig. 1 depict the observed variations with composition of the fundamental band gap¹⁴ [Fig. 1(a)] and bond lengths¹⁵ [Fig. 1(b)] in the $\text{Cd}_{1-x}\text{Mn}_x\text{Te}$ alloy. Expectations based on similar measurements in "normal" semiconductor alloys¹

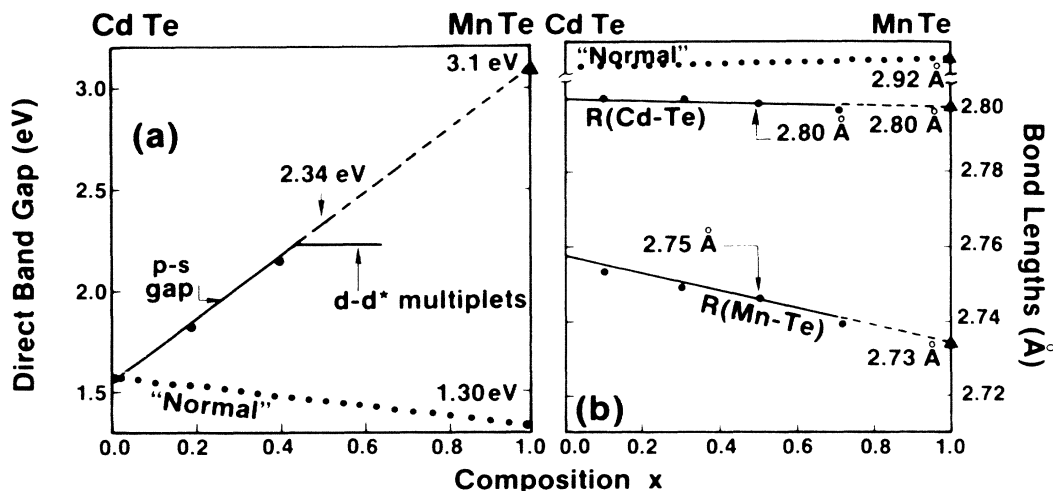


FIG. 1. Observed variations with composition x of (a) the fundamental band gap (Ref. 14), and (b) bond lengths (Ref. 15) in $\text{Cd}_{1-x}\text{Mn}_x\text{Te}$. Dashed lines are extrapolations; dotted lines are expectations for "normal" isovalent alloys.

(types I and II above) suggest (dotted lines in Fig. 1) that as Mn is added to CdTe the band gap will *decrease* (with a possible bowing), approaching the smaller value of MnTe, and the Mn—Te bond length will either *increase* slightly,² or stay nearly constant² around its value of 2.92 Å in MnTe. Experimental observations^{14,15} (Fig. 1) indicate instead that the opposite is true: For compositions below $x=0.7$, for which single-phase samples can be prepared,^{7,14} the band gap *increases* and the Mn—Te bond length *decreases* slightly with added Mn. A rough extrapolation of the data from $x \leq 0.42$ to $x=1$ (dashed lines in Fig. 1) suggests a “limiting MnTe phase” with $E_g \approx 3.1$ eV and $R(\text{Mn—Te}) \approx 2.73$ Å. A similar extrapolation for⁷ $\text{Hg}_{1-x}\text{Mn}_x\text{Te}$ also gives similar values of $E_g \approx 3.3$ eV and $R(\text{Mn—Te}) \approx 2.74$ Å. The differences between the properties of this “limiting MnTe phase” and those of normal^{10,11} MnTe are so dramatic that we are inclined to think that this phase corresponds to a hitherto unknown new structure of MnTe, with fundamentally new properties.

To clarify the properties that such a material might have, we have performed self-consistent, local-density, spin-polarized total-energy and band-structure calculations for a few phases of MnTe with Bravais lattices similar to those observed for the alloy.¹⁵ We use the semirelativistic general-potential linear augmented plane-wave method¹⁶ with the Von Barth–Hedin exchange-correlation potential, muffin-tin radii of 2.53 a.u. for all atoms, and about 90 basis functions per atom. The uncertainty in the calculated total-energy differences for the cubic phases is estimated to be about 0.05 eV, and about 0.1 eV when compared to the hexagonal phase. Figure 2 depicts the calculated variations with bond length of the total energies of ferromagnetic (F) and antiferromagnetic (AF) MnTe in the zinc-blende (ZB) structures (inset to Fig. 2). We find as follows: (i) The AF phase is stabler than the F phase by 0.19 eV/atom-pair; the two phases have similar bond lengths of $R(\text{Mn—Te}) = 2.70 \pm 0.02$ Å, close to the value of 2.73 Å extrapolated from the experimental data [Fig. 1(b)] for the “limiting phase.” (ii) While these phases have substantial cohesion relative to free atoms (7.37 and 7.56 eV/atom-pair for the F and AF phases, respectively), we calculate that the *observed* AF-NiAs structure is stabler by 0.40 and 0.21 eV/atom-pair relative to the zinc-blende F and AF forms, respectively. Hence, we would not expect to find the isolated ZB phase under conditions where equilibration to the NiAs form is not hindered by activation barriers. (iii) While the absolute value of local spin-density band gaps cannot be meaningfully compared with experiment, the *relative differences* in the gaps are far more realistic.¹⁷ We calculate that the ZB phases of MnTe have a $p \rightarrow s$ band gap that *exceeds* that calculated for CdTe by 2.1 eV (and $p-d$ and $d-d$

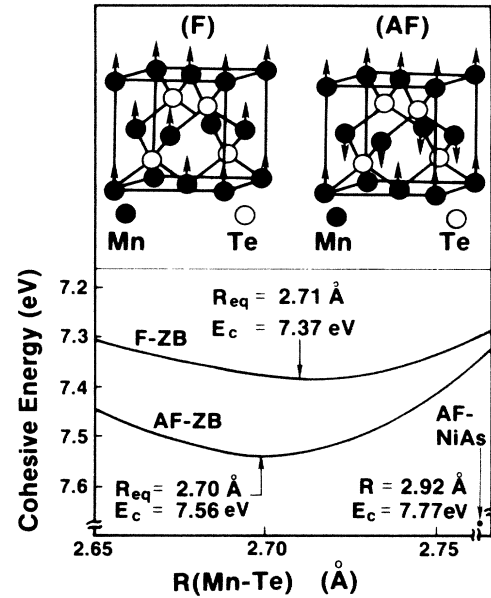


FIG. 2. Cohesive energy as function of zinc-blende lattice parameter for F and AF MnTe. The calculated result for the observed AF MnTe in the NiAs structure is also shown (solid circle). The upper portion depicts the spin ordering in these two phases.

gaps that are 0.9 eV larger than MnTe in the NiAs structure; see below).

Our calculations hence suggest the possibility of a cubic phase of MnTe with properties which are similar to those inferred for the “limiting phase” from the data on $\text{Cd}_x\text{Mn}_{1-x}\text{Te}$. Such a phase is predicted, however, to be metastable when isolated in bulk form. Can this metastability barrier be lowered in the alloy? To address this question we have performed similar calculations for the $\text{Cd}_{0.5}\text{Mn}_{0.5}\text{Te}$ alloy in the ordered CuAu-I ferromagnetic structure, i.e., CeMnTe_2 . In addition to its cubic lattice constant a , the CuAu-I structure² has an internal structural degree of freedom, i.e., the anion displacement parameter, given by $u = \frac{1}{4} + (R_{AC}^2 - R_{BC}^2)/a^2$, measuring the possible mismatch in the two bond lengths R_{AC} and R_{BC} in the unit cell (i.e., Mn—Te and Cd—Te). We have minimized the total energy $E(\text{CdMnTe}_2, a, u)$ as a function of u and a , finding at equilibrium $a_{\text{eq}} = 6.37$ Å and $u_{\text{eq}} = 0.242$. These values correspond to $R(\text{Mn—Te}) = 2.73$ Å and $R(\text{Cd—Te}) = 2.79$ Å, which are within 1% of the values observed for the 50%–50% alloy in extended x-ray absorption fine-structure measurements¹⁵ [arrows in Fig. 1(b)]. The fact that these values are also close to those of the pure end-point compounds suggests that the system has used its internal degree of freedom u to achieve nearly ideal bond lengths, thereby lowering its strain energy.^{2a} Evaluating the enthalpy of formation (per four atoms) for the ferromagnetic phases relative to

the equilibrium ZB forms of CdTe and F-MnTe,

$$\Delta H = E(\text{CdMnTe}_2, a_{\text{eq}}, u_{\text{eq}}) - E(\text{CdTe}) - E(\text{MnTe})$$

we find a *negative* value of $\Delta H = -0.05$ eV. Hence, the CuAu-I phase of F-CdMnTe₂ is predicted to be stable against disproportionation into its ZB constituents. Whereas AF-CdMnTe₂ has even a lower total energy than F-CdMnTe₂, it is unstable with respect to AF-MnTe + CdTe by at least 0.04 eV, suggesting the possibility of clustering of the Mn-rich alloy into domains of AF-MnTe. While the F or AF alloy is still less stable relative to the NiAs structure, coherent strain activation barriers,^{2a} posed by the large lattice relaxation needed to transform the ZB structure to the NiAs structure, suggest that, once formed, the ZB phase may persist. Furthermore, recent theoretical studies on epitaxial confinement^{9b} suggest that if the ZB phase is grown on a substrate with a different lattice constant, substrate strain effects may further stabilize it. Experimental attempts to grow and characterize these structures are called for.

In Fig. 3 we show the calculated band structures of ferromagnetic CdMnTe₂; we find that the spin-up Mn *d* band is occupied, centered at $E_v^\uparrow - 3.7$ eV [Fig. 3(a), where E_v^\uparrow is the top of the valence band for spin up], whereas the spin-down *d* band is empty, centered at $E_v^\downarrow + 2.9$ eV [Fig. 3(b)]. The +4.9-eV separation between them constitutes the effective *d*-band exchange (*x*) splitting $\Delta_x(d)$. Remarkably, we find that the *p-d* exchange splitting $\Delta_x(pd) = E_v^\downarrow - E_v^\uparrow$ of the

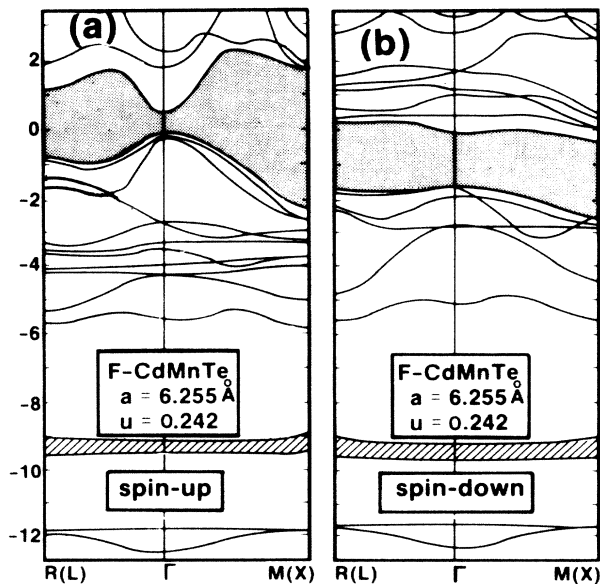


FIG. 3. Electronic band structure of F-CeMnTe₂ (a and b). The zero of the energy is at E_v^\uparrow . Symbols in parenthesis are the points of fcc Brillouin zone.

top of the valence band is *negative*: The top of the valence band for spin up (E_v^\uparrow , having in the muffin-tin spheres 20% Mn *d* and $2 \times 24\%$ Te *p* character) is 1.7 eV *above* the top of the valence band for spin down (E_v^\downarrow , with 22% Mn *d* and $2 \times 21\%$ Te *p* character). This is at first surprising, given the fact that we find the effective potential for the majority spin to be more attractive than that for the minority spin, as is usually the case in spin-polarized systems.¹⁸ Figure 4 explains this phenomenon in terms of a simple *p-d* repulsion model.¹⁷ What is special about Mn and Te (as well as Mn-S and Mn-Se) is that the calculated atomic *p* \uparrow and *p* \downarrow orbital energies of the anion are bracketed by the atomic *d* \uparrow and *d* \downarrow levels of Mn (Fig. 4). In the tetrahedral crystal field, the anion *p* states have the t_2 (Γ_{15}) symmetry and the metal *d* states are split into a doublet with *e* (Γ_{12}) symmetry and a triplet with t_2 (Γ_{15}) symmetry; the *e* states are lower than the t_2 states, there is no *p-d* hybridization between them. On the other hand, the coupling between the spin-up states with the same t_2 symmetry produces a lower bonding (B_+) and a higher antibonding (AB_+) levels; the coupling between the spin-down states with the same t_2 symmetry produces similarly a lower bonding (B_-) and a higher antibonding (AB_-) pair. Since the unperturbed *d* \uparrow is below *p* \uparrow , but *d* \downarrow is above *p* \downarrow , simple perturbation theory leads to the situation where B_- is below AB_+ , and hence an effective *negative* *pd* exchange splitting. This *p-d* coupling mechanism, used previously¹⁷ to explain the anomalously small band gaps of ternary 3*d* semiconductors, suggests also here a smaller spin-up band gap (calculated: 0.63 eV) than the spin-down band gap (1.64 eV). The same phenomenon occurs for F-MnTe. This covalent *p-d* hybridization is also found to reduce the local

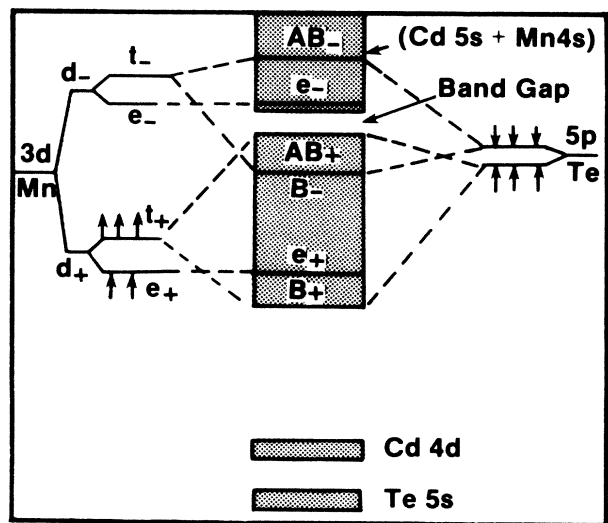


FIG. 4. Schematic diagram of the *p-d* repulsion effect, for ferromagnetic CdMnTe₂.

magnetic moment of Mn from its free-space value of $5.0\mu_B$ to $4.30\mu_B$, and even produces a small local magnetic moment of $0.09\mu_B$ and $0.05\mu_B$ on the otherwise nonmagnetic Te and Cd sites, respectively. In the AF spin arrangement the negative p - d exchange splitting will disappear. This is because there are equal numbers of Mn atoms with $3d$ levels below and above the Te p levels; the latter are repelled equally by $d \uparrow$ and $d \downarrow$, and hence no exchange splitting occurs for Te p states. Furthermore, since the $p \uparrow$ - $d \uparrow$ hybridization is stronger than the $p \downarrow$ - $d \downarrow$ hybridization, the difference in spin symmetry between the F and AF phases also indicates the enhanced stability of the AF structure: the stronger p - d repulsion in the F phase reduces the cohesion of the p bands.

The reason that the band gap of CdTe increases upon addition of Mn [Fig. 1(a)] with almost zero bowing can be simply explained in terms of the limiting phase being ZB rather than NiAs. We find the calculated interband p - s transition energy to be 1.43 eV; this is close to the average (1.48 eV) of our calculated p - s energies of the end-point compounds, i.e., $E^{p-s}(\text{CdTe}) = 0.44$ eV and $E^{p-s}(\text{F-MnTe}) = 2.53$ eV, suggesting a vanishing optical bowing. We conclude that the initial increase of the band gap of CdTe with added Mn [Fig. 1(a)] is due to the interband p - s transition. When the Mn concentration is increased, the conduction cation s states recede to higher energies relative to the Mn $3d \downarrow$ states (which, being more localized, are not as sensitive to composition changes); hence the excitations will then acquire a Te, $p \rightarrow \text{Mn } d \downarrow$ character with large atomiclike multiplet effects.

The exchange-interaction coefficients can be estimated from our first-principles total-energy and band-structure calculation. The calculated nearest-neighbor interaction energy J_{nn} between the localized Mn magnetic moments is found to be -16 K at the calculated lattice constant and -15 K at the extrapolated lattice constant.¹⁵ The exchange constants $N_0\alpha$ and $N_0\beta$, which are responsible for the unique properties of $\text{Cd}_{1-x}\text{Mn}_x\text{Te}$,¹⁹ are found to be 0.41 and -1.09 , respectively. These are in satisfactory agreement with experiments^{19,20} and a recent theoretical calculation.²¹

In summary, our calculation indicates that the alloy environment stabilizes a hitherto unknown ZB phase of MnTe and that in its ferromagnetic form it has a negative p - d exchange splitting and small magnetic moments even on the nonmagnetic ions (Cd, Te). The exchange-interaction coefficients have been estimated from our *first-principles* calculations.

The authors would like to acknowledge helpful conversations with D. M. Wood. This work was supported by the Office of Energy Research, Materials Science

Division, U.S. Department of Energy, Grant No. DE-AC02-77-CH00178.

¹J. C. Woolley, in *Compound Semiconductors*, edited by R. K. Willardson and H. L. Goering (Reinhold, New York, 1962), p. 3.

^{2a}G. P. Srivastava, J. L. Martins, and A. Zunger, *Phys. Rev. B* **31**, 2561 (1985).

^{2b}T. S. Kuan, T. F. Kuech, W. I. Wang, and E. L. Wilkie, *Phys. Rev. Lett.* **54**, 201 (1985).

³A. G. Fisher and R. J. Paff, *J. Phys. Chem. Solids* **23**, 1479 (1962).

⁴A. F. Bolshakov, A. O. Dmitrenko, and B. V. Abalduev, *Inorg. Mater. (U.S.S.R.)* **15**, 1189 (1979).

⁵A. D. Stuckers and G. Farrell, *J. Phys. Chem. Solids* **25**, 477 (1964).

⁶A. Kalb and V. Leute, *Phys. Status Solidi (a)* **5**, K199 (1971).

⁷R. Juza, A. Rabenau, and G. Pascher, *Z. Anorg. Allg. Chem.* **285**, 61 (1956); J. Kaniewski, W. Szuskiewicz, and A. Mycielski, *Pr. Inst. Fiz. Pol. Akada Nauk.* **74**, 34 (1977); R. T. Delves and B. J. Lewis, *J. Phys. Chem. Solids* **24**, 549 (1963).

⁸J. L. Zilko and J. E. Green, *J. Appl. Phys.* **51**, 1549 (1980).

^{9a}A. Ourmazd and J. C. Bean, *Phys. Rev. Lett.* **55**, 765 (1985).

^{9b}J. L. Martins and A. Zunger, *Phys. Rev. Lett.* **56**, 1400 (1986).

¹⁰W. D. Johnston and A. E. Sestrich, *J. Inorg. Nucl. Chem.* **19**, 229 (1961).

¹¹J. W. Allen, G. Lucovsky, and J. C. Mikkelsen, *Solid State Commun.* **24**, 367 (1977).

¹²D. J. Chadi, J. P. Walter, M. L. Cohen, Y. Petroff, and M. Balkanski, *Phys. Rev. B* **5**, 3058 (1972).

¹³L. Tomassen, D. R. Mason, G. D. Rose, J. C. Sarace, and G. A. Schmitt, *J. Electrochem. Soc.* **110**, 1127 (1963).

¹⁴N. T. Khoi and J. A. Gaj, *Phys. Status Solidi (b)* **83**, K133 (1977).

¹⁵A. Balzarotti, M. Czyzyk, A. Kisiel, N. Motta, M. Podgorny, and M. Zimnal-Starnawska, *Phys. Rev. B* **30**, 2295 (1984).

¹⁶S.-H. Wei, H. Krakauer, and M. Weinert, *Phys. Rev. B* **32**, 7792 (1985).

¹⁷J. E. Jaffe and A. Zunger, *Phys. Rev. B* **29**, 1882 (1984).

¹⁸V. L. Morozzi, J. F. Janak, and A. R. Williams, *Calculated Electronic Properties of Metals* (Pergamon, New York, 1978).

¹⁹J. A. Gaj, R. Paniel, and G. Fishman, *Solid State Commun.* **29**, 435 (1979).

²⁰T. M. Giebultowicz, J. J. Rhyne, W. Y. Ching, and D. L. Huber, *J. Appl. Phys.* **57**, 3415 (1985).

²¹B. E. Larson, K. C. Hass, M. Ehrenreich, and A. E. Carlsson, *Solid State Commun.* **56**, 347 (1985); K. C. Hass, B. E. Larson, H. Ehrenreich, and A. E. Carlsson, *J. Magn. Mater.* **54-57**, 1283 (1986).

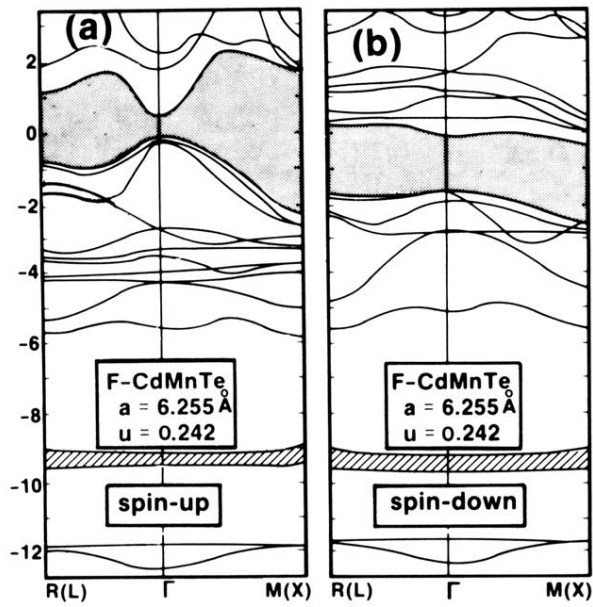


FIG. 3. Electronic band structure of F-CeMnTe₂ (a and b). The zero of the energy is at E_v^{\uparrow} . Symbols in parenthesis are the points of fcc Brillouin zone.

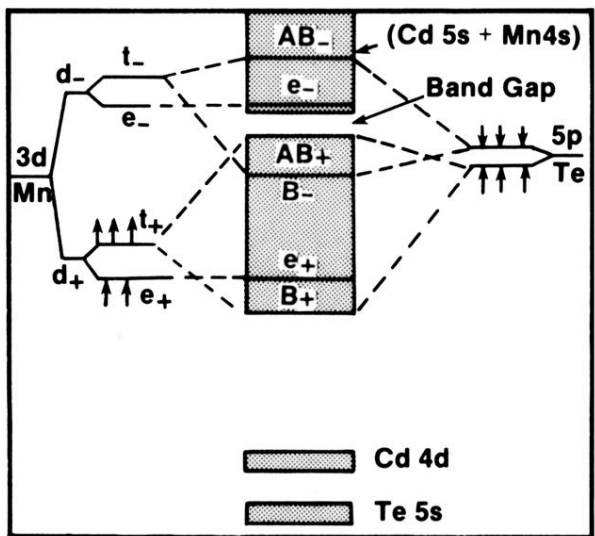


FIG. 4. Schematic diagram of the *p-d* repulsion effect, for ferromagnetic CdMnTe₂.